

Transient sliding of thin hydrogel films: the role of poroelasticity
Lola Ciapa, Jessica Delavoipière, Yvette Tran, Emilie Verneuil and Antoine Chateaubinois
Supplementary Information

Numerical resolution of the poroelastic contact model for $Pe > 1$.

We describe here the numerical resolution of Eqns (19,23) and (35) for the contact pressure $\bar{\sigma}(r, \theta)$, the pore pressure field $\bar{p}(r, \theta)$, and the friction force F_t , respectively, when $Pe > 1$. In this Péclet regime, the contact is no longer circular as a result of the pore pressure imbalance generated by advection. An additional unknown of the poroelastic contact problem is thus the contact shape. Here, we make the assumption that the contact line has the general form $\bar{r} = \bar{\rho}(\theta)$ where $\bar{\rho} = \rho/a$ is an even function of θ . Consistently with the experimental observation reported in Delavoipière *et al*¹, the contour line ρ is assumed to be described by an ellipse for $|\theta| \geq \pi/2$ while the leading edge of the contact remains circular ($|\theta| \leq \pi/2$).

$$\begin{aligned} r &= a \quad |\theta| \leq \pi/2 \\ r^2 \cos^2 \theta + \frac{r^2 \sin^2 \theta}{\zeta^2} &= a^2 \quad |\theta| \geq \pi/2 \end{aligned} \quad (\text{SI.1})$$

which can be recast in a non dimensional form:

$$\begin{aligned} \bar{r} &= 1 \quad |\theta| \leq \pi/2 \\ \bar{r}^2 \cos^2 \theta + \frac{\bar{r}^2 \sin^2 \theta}{\zeta^2} &= 1 \quad |\theta| \geq \pi/2 \end{aligned} \quad (\text{SI.2})$$

where $0 < \zeta < 1$ is a numerical parameter describing the contact asymmetry.

For each Péclet number Pe^0 , the three unknowns \bar{a} , ζ and \bar{a} have to be determined as a function of the reduced time $\bar{t} = t/\tau$. The solution of the contact problem should comply to the following boundary conditions:

1. the pore pressure $\bar{p}(\bar{r}, \theta)$ is vanishing at the contact edge (cf eqn (20)),
2. the contact stress $\bar{\sigma}(\bar{r}, \theta)$ should fulfill eqn (21), i.e

$$\int \int_A \bar{\sigma} dA = \frac{\pi}{2\bar{a}^2} \quad (\text{SI.3})$$

where A is the actual contact.

3. We also enforce the condition that the contact stress $\bar{\sigma}$ cannot be negative at the edge of the contact, otherwise it will open: indeed, adhesion is not expected to be significant with the contact fully immersed within water, and adhesive forces are not accounted for in the model. However, negative (suction) contact stresses are allowed within the contact area provided that $\bar{\sigma}$ remains positive over a prescribed reduced length $\bar{w} = w/a_0$ at the edge of the contact (see Fig. SI1). Here, we enforce the criterion $\bar{w} \geq 0.01$ which corresponds to the thickness of the hydrogel layer used in the experiments (i.e. $w/e_0 \approx 1$).

Steady-state sliding

For steady-state sliding, $\bar{a} = 0$ and the problem reduces to the determination of \bar{a} and ζ . For each of the considered Pe number, we start from the calculation of the pore pressure and contact stress fields for various combinations of \bar{a} and ζ within the range $0.4 < \bar{a} < 1$ and $0.5 < \zeta < 1$. For each (\bar{a}, ζ) doublet, we determine the set of α_n parameters ensuring $\bar{p} = 0$ on the considered contact line defined by Eq.SI.2. Once α_n are determined, \bar{p} and $\bar{\sigma}$ can be calculated everywhere in the contact area using eqns (19,23). Then, we search in the discretized (\bar{a}, ζ) space the solution which obeys the second and third boundary conditions.

The calculated $\bar{a}(Pe^0)$ and $\zeta(Pe^0)$ solutions are shown in Fig. SI2(a) together with some

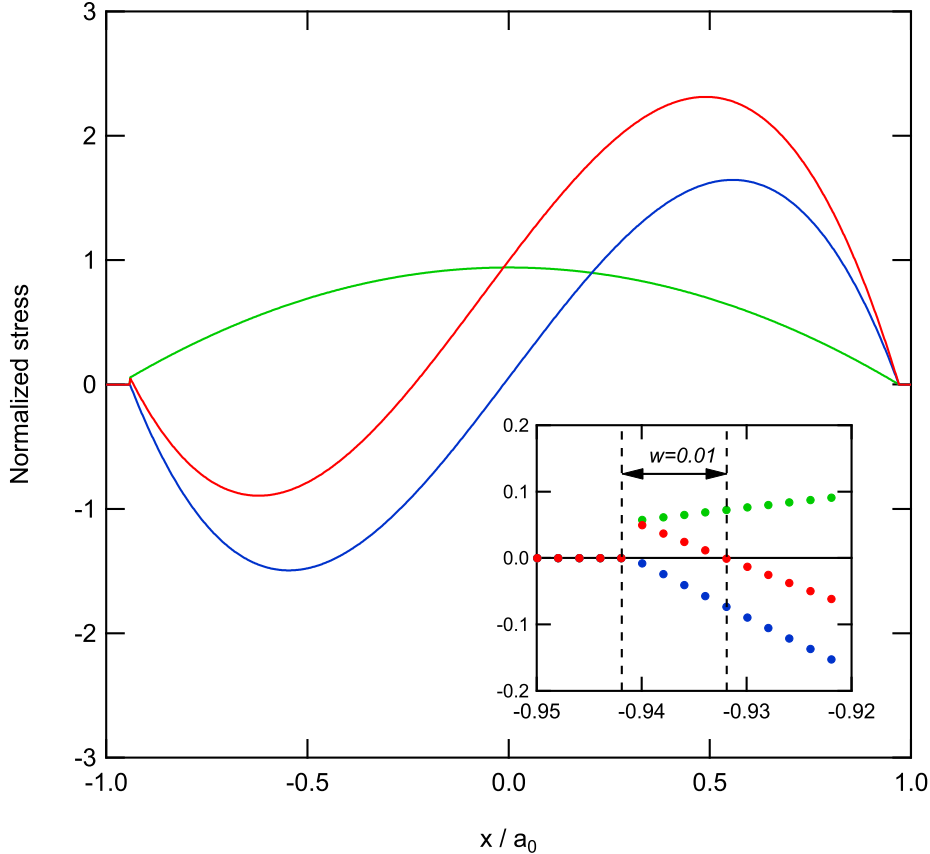


Figure SII: Profiles of the calculated pore pressure \bar{p} (blue), contact stress $\bar{\sigma}$ (red) and elastic stress $\sigma_e = (1 - \bar{p})\bar{a}^2$ (green) along the sliding direction x ($y = 0$). Inset: details of the profiles at the leading edge of the contact where $\bar{w} = 0.01$ is the normalized width over which the contact stress $\bar{\sigma}$ remains positive from the edge of the contact.

experimental data taken from Delavoipière *et al*¹ and from the present study. In Fig. SI2(b), the calculated F_t/F curve has been shifted vertically to fit the experimental data as the expression of the friction force is derived from a scaling argument (eqn (28)) with an unknown prefactor. The maximum in friction force occurs for a Pe^0 greater than unity ($Pe^0 \approx 8$) as a result of two competing effects (*i*) the increase in viscous dissipation per unit film volume within the contact as Pe^0 is increased, (*ii*) the decrease in the size of the contact, i.e. in the film volume affected by poroelastic flow.

For the highest Pe value achieved in the transient experiments of this paper (i.e. $Pe = 6$), the calculated contact asymmetry ($\zeta = 0.966$) is very close to unity, in agreement with the

experimental observation that the contact remains nearly circular within optical resolution.

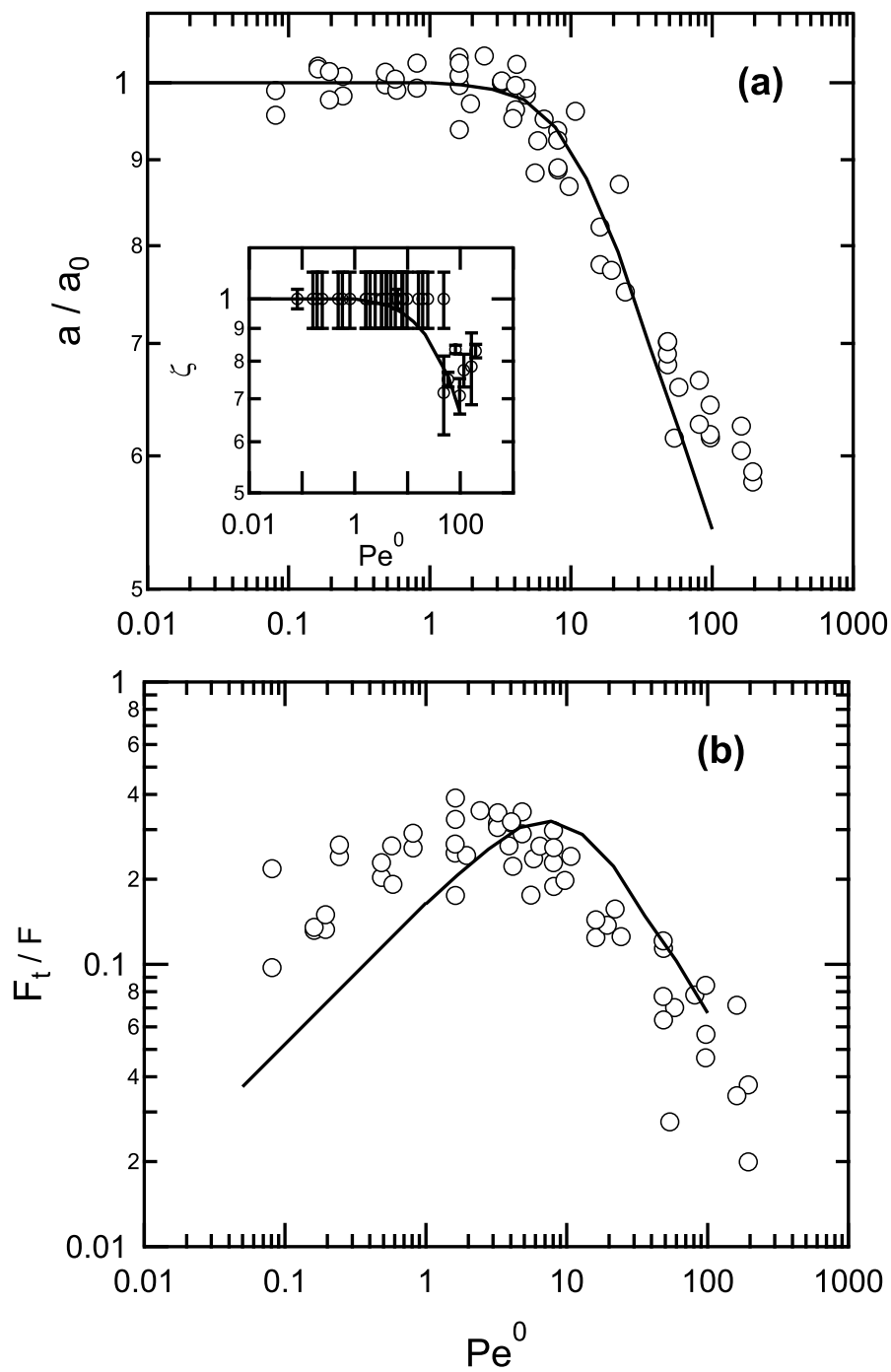


Figure SI2: Numerical (solid line) and experimental (open symbols) (a) contact shape (\bar{a}, ζ) and (b) reduced friction force F_t/F as a function of Pe^0 . Open symbols corresponds to experimental data for PDMA films taken from the present study and Delavoipière *et al*¹.

Transient sliding

For transient sliding, along the same lines we calculate the contact stresses in a discretized (\bar{a}, ζ) space for the considered Pe number and a discretized set of \bar{a} values ranging from the initial (\bar{a}_i) to the steady-state (\bar{a}_s) contact radii. For each value of \bar{a} , and in the (\bar{a}, ζ) space, we determine the solution which satisfies the three above mentioned boundary conditions. The reduced time increment $\Delta\tau$ separating to successive contact radius values is determined as

$$\Delta\tau = \frac{\bar{a}_{n+1} - \bar{a}_n}{\bar{a}_{n+1}} \quad (\text{SI.4})$$

An example of the calculated $a(t)$ is shown in Fig. SI3 for $Pe = 6$ and two different initial contact radii, together with the corresponding experimental data, and is found to be in fair agreement.

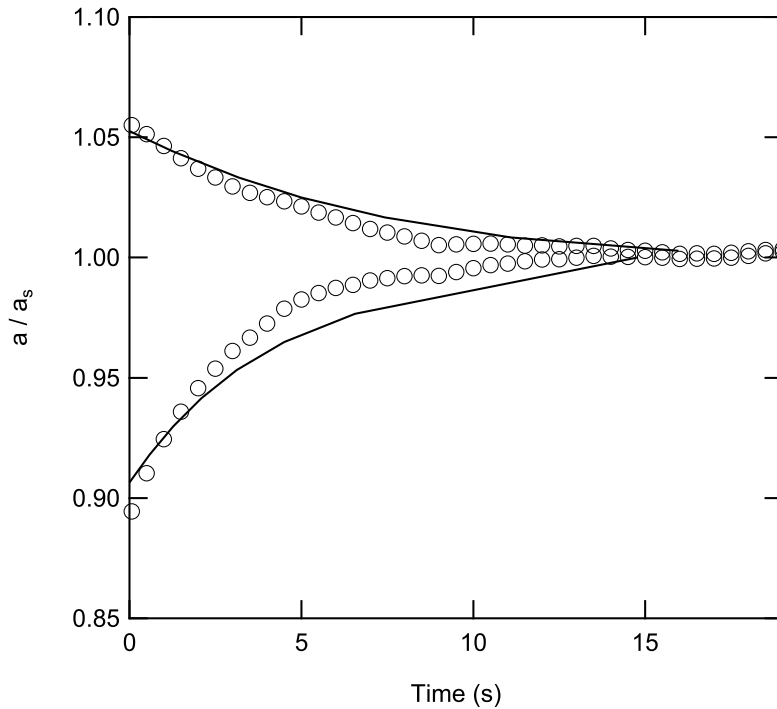


Figure SI3: Numerical (solid lines) and experimental (open symbols) $a(t)$ kinetics for $Pe = 6$ and two different values of the initial contact area ($a/a_s = 0.89, a/a_s = 1.05$).

Equivalent force F_{eq}

In order to provide an approximate solution for the transient at $Pe > 1$, we made the assumption that an effective load $F_{eq} = F - F_{lift}$ smaller than the imposed load F is applied to the contact as a result of the lift force F_{lift} generated by the pore pressure imbalance. The effective load was approximated from the steady-state contact radius a_s under the assumption that the contact remains nearly circular (eqn (33)). It is therefore taken as constant during the transient.

Here, the numerical simulation allows to calculate the time-dependence of this effective load while taking into account the actual non-circular shape of the contact. Note that, consistently with the non-dimensional variables used in the paper, all forces are normalized by $2F/\pi$. The lift

force arises from the advective component of pore pressure (eqn (22)). Hence, the normalized expression of the applied load \bar{F} , the lift force \bar{F}_{lift} , the effective load \bar{F}_{eq} write:

$$\begin{aligned}\bar{F} &= \pi/2 \\ \bar{F}_{lift} &= \int \int_A \bar{a}^2 \bar{p}^o \bar{r} d\bar{r} d\theta \\ \bar{F}_{eq} &= \int \int_A \bar{a}^2 (\bar{\sigma} - \bar{p}^o) \bar{r} d\bar{r} d\theta\end{aligned}\tag{SI.5}$$

Using eqn (23), \bar{F}_{eq} simply writes:

$$\bar{F}_{eq} = \bar{a}^4 \int \int_A (1 - \bar{r}^2) \bar{r} d\bar{r} d\theta\tag{SI.6}$$

In the numerical model, the contact line is assumed to be circular at the leading edge and elliptic at the trailing edge (Eq. SI.2). Under this assumption, an analytical expression of \bar{F}_{eq} can be derived as a function of \bar{a} and ζ :

$$\bar{F}_{eq} = \frac{\pi}{2} \bar{a}^4 \frac{1}{2} \left(1 + \frac{\zeta}{2} (3 - \zeta^2) \right)\tag{SI.7}$$

In the limit of small contact assymetry, ζ is close to 1 and the effective load in Eq.SI.7 amounts to the approximation made in eqn (33): $\bar{F}_{eq} \sim \pi \bar{a}^4 / 2$.

The equivalent force \bar{F}_{eq} has been calculated for various Pe numbers, either starting from the indentation equilibrium *i.e.* $a = a_0$ and $\bar{a} > 1$ or starting from a value smaller than the steady state contact radius *i.e.* $\bar{a} < 1$. In Fig. SI4, the results were reported as a function of the time-dependent normalized contact radius $\tilde{a} = a(t)/a_s$ achieved at the various stages of the transient, where a_s is the steady-state contact radius. It can be seen that, starting from a_i smaller or larger than a_s , \bar{F}_{eq} is respectively slowly decreasing or increasing toward the limit corresponding to $\bar{F}_{eq} \sim \pi \bar{a}_s^4 / 2$ (eqn (33)) as a reaches its steady state value ($\tilde{a} \rightarrow 1$) *i.e.* toward the frictional equilibrium. The amplitude of this change is enhanced when Pe is increased. However, the hypothesis of constant effective load during the transient is acceptable for $Pe \leq 6$: this supports the assumptions made in the derivation of an approximate analytical solution for the time variations of the contact radius a (eqn (34)).

References

- [1] J. Delavoipière, Y. Tran, E. Verneuil, B. Hertefeu, C.-Y. Hui and A. Chateauminois, *Langmuir*, 2018, **34**, 9617–9626

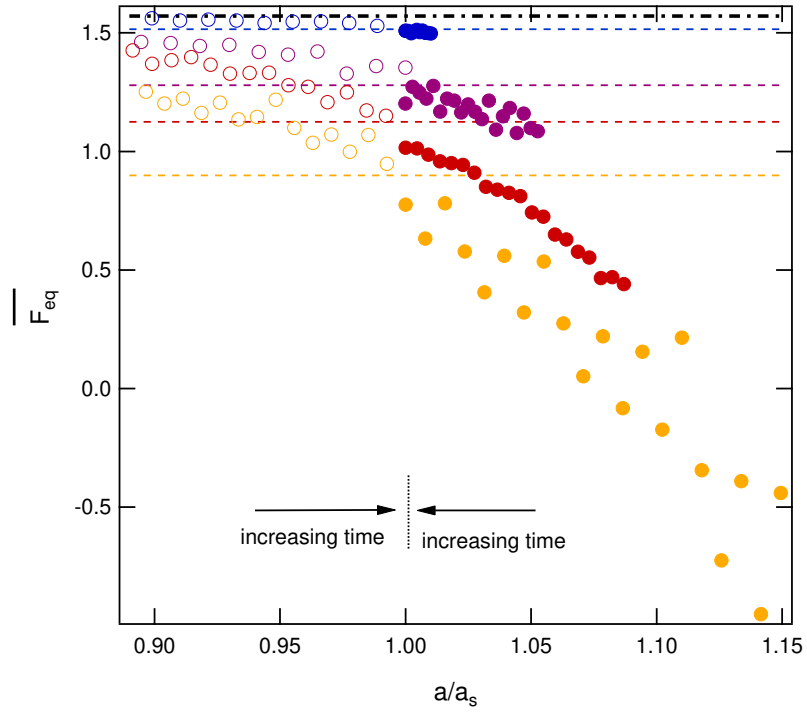


Figure SI4: Calculated normalized equivalent force \overline{F}_{eq} as a function of a/a_s for various values of the Péclet number. Blue: $Pe = 3$; Purple: $Pe = 6$; Red: $Pe = 10$; Yellow $Pe = 15$. Open and filled symbols correspond respectively to initial values of a/a_s smaller and larger than 1. The horizontal dotted lines correspond to $\overline{F}_{eq} = \pi \overline{a}_s^4/2$. The dash dotted line correspond to the normalized applied normal load $\overline{F} = \pi/2$.